Exchange biasing of a Néel wall in the nanocontact between NiFe wires

K. Miyake[a)]
Institute for Chemical Research, Kyoto University, Uji, Kyoto 611-0011, Japan

K. Shigeto
RIKEN, Wako, Saitama 351-0198, Japan

Y. Yokoyama
Nano-electronics Research Institute, National Institute of Advanced Industrial Science and Technology, Tsukuba 305-8568, Japan

T. Ono
Graduate School of Engineering Science, Osaka University, Toyonaka, Osaka 560-8531, Japan

K. Mibu
Research Center for Low Temperature and Materials Sciences, Kyoto University, Uji, Kyoto 611-0011, Japan

T. Shinjo
International Institute for Advanced Studies, Kizu, Kyoto 619-0225, Japan

(Received 17 September 2003; accepted 13 October 2004; published online 14 December 2004)

We fabricated nanocontact structures (typically in a range from 15×13 nm^2 to 20×40 nm^2) between $Ni_{81}Fe_{19}$ wires using electron-beam lithography and a lift-off process. In the magnetization reversal process for each sample, two kinds of magnetic domain walls with different magnetic configurations were trapped at the nanocontact between the two wires. The directions of the magnetization in the nanocontact were different between the two domain walls. These walls yielded different values of electric resistance and different depinning fields. The magnetization of the nanocontact suppresses or assists the magnetization rotation in the connected magnetic element through exchange interaction (exchange biasing), which causes the differences in the depinning field and dominates the magnetization process of the magnetic element. © *2005 American Institute of Physics*. [DOI: 10.1063/1.1829143]

I. INTRODUCTION

The magnetization configurations and the magnetization reversal processes in patterned elements of submicron size, made of magnetic films, can be varied by controlling the sample shape. The spin configuration of a magnetic domain wall (DW) can also be varied by controlling the sample shape. The DW width generally depends on the exchange stiffness constant and the magnetocrystalline anisotropy or shape anisotropy. However, the condition changes if the magnet has a very small constriction. It has been theoretically predicted that the DW in a small constriction becomes as small as the size of the constriction.[1,2] On the other hand, a large magnetoresistance (MR) ratio was experimentally observed for a point contact between macroscopic ferromagnetic metals[3] and oxides.[4] The large change in resistance is considered to be due to the formation of a DW at the point contact, where the spin rotation ends for several atoms. However, the type of spin configuration of the DW confined to the point contact has not been confirmed experimentally. In this article, we report the magnetic structures and properties of the DW in a nanocontact between $Ni_{81}Fe_{19}$ wires, which were fabricated using electron-beam lithography and a lift-off process. We observed four kinds of DWs with two different depinning fields in a series of samples using magnetic force microscopy (MFM) observations. We also observed two kinds of magnetization processes in each sample using MR measurements. It was found that these differences in the magnetization processes arise from the differences in the directions of magnetization in the nanocontact.

II. SAMPLE PREPARATION

We developed a nanocontact structure between two $Ni_{81}Fe_{19}$ wires with different widths (340 and 180 nm) and a thickness of 10 nm. Figure 1 shows a schematic illustration of a typical sample and a scanning electron microscopy (SEM) image of the area around the nanocontact. The samples were patterned on thermally oxidized Si substrates using electron-beam lithography with ZEP520-22 resist, e-gun deposition in a vacuum of 1×10^{-8} Torr at room temperature, and a lift-off process with 2-butanone. We estimated the nanocontact size from the SEM image to be 15×13 nm^2. Such a small contact size was realized in the following manner. Several samples with different designed distances between two wires were patterned on the same substrate. Incidentally, we obtained extremely small contact structures among these samples. The size of the contact depends on the sharpness of the tip structure of the two wires. So far, we have fabricated a contact size as small as 15×13 nm^2 using the finest resolution of the electron-beam

a)Author to whom correspondence should be addressed; electronic mail: miyake@ssc1.kyoto-u.ac.jp

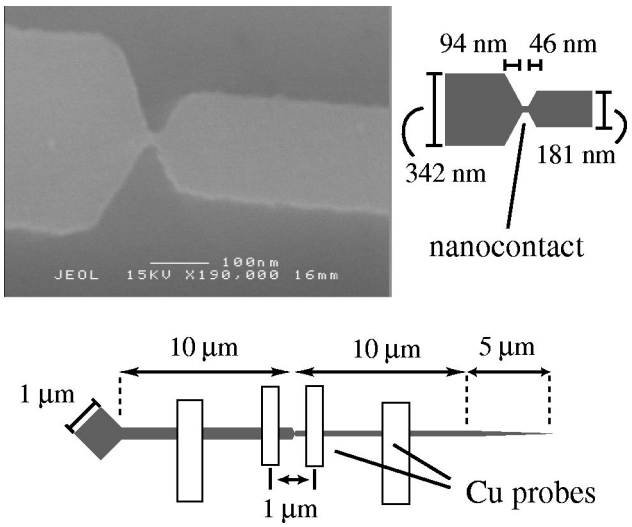

FIG. 1. Schematic illustration of the shape of a typical sample and the SEM image of the nanocontact between two wires. The narrowest square between two wires is defined as "nanocontact" in this article. The size of the nanocontact estimated from the SEM image was 15×13 nm^2.

lithography system. A pad was attached at the end of the wider wire, and the narrower wire was sharply pointed. These particular shapes were introduced in order to control the direction of the DW injection. When a magnetic field is applied parallel to the wire axis, a DW is injected from the pad and the magnetization reversal takes place in the wider wire.[5] The DW is depinned from the nanocontact when the magnetic field reaches the coercive field of the narrower wire. The sharply pointed structure prevents the nucleation of another DW from this end.[6] In this manner, the magnetization process is characterized by the two critical fields corresponding to the DW injection field from the pad and the depinning field from the nanocontact when the magnetic field is applied parallel to the wire axis. The magnetization process was confirmed experimentally using Kerr microscopy observations[7] for samples with different sizes and an identical shape.

III. EXPERIMENTS

MFM observations were performed in a vacuum of 1×10^{-5} Torr using a SPI-3800N system from Seiko Instruments Incorporation. Low-moment probes of CoPtCr were used in order to avoid the influence of stray fields from the probe.

The MR effect was measured by a dc four-probe method using physical property measurement system (PPMS) from Quantum Design. The current and voltage probes used on the samples consisted of a nonmagnetic material, Cu, with a thickness of 20 nm. The distance between the voltage probes was 1 μm (Fig. 1). A current of 20 μA, which is small enough to not cause a DW motion by the spin injection,[8,9] was used for the measurements.

The magnetic structures around the nanocontact were calculated using the micromagnetics simulation on the basis of the Landau–Lifshiz–Gilbert equation. A unit-cell size of 2.5×2.5 nm^2 with a constant thickness of 10 nm, magnetization of 1.08 T, and a damping parameter $\alpha=1.0$ were used for the calculation. Since the number of meshes used for calculation is limited by the finite memory of the computer, the calculation was carried out under the following boundary conditions. The magnetization directions of both ends of the simulated area were fixed along the wire axis, so that the magnetic charges of the end of the wires were not considered in this calculation.

IV. RESULTS AND DISCUSSION

A. MFM observations

The DWs trapped at the nanocontacts were observed using MFM at room temperature. The sizes of the observed nanocontacts were in the range from 15×13 nm^2 to 20×40 nm^2. Figure 2(a) shows the MFM image at zero field after applying a field of −400 Oe. We can see two types of signals in the image (white signals at the edge of the wider wire and black signals at the edge of the narrower wire) originating from the different magnetic charges. The image shows that the magnetizations of the wires are parallel to the wire axis up to the edge and a DW does not exist at the nanocontact. Two types of DWs were then found to be trapped at the nanocontact when a field sweep of −400 Oe $\rightarrow$ +100 Oe $\rightarrow$ 0 Oe was repeated for the same sample (Figs. 2(b) and 2(c)). Dark signals were observed at the edges of the two wires in the images in Figs. 2(b) and 2(c), indicating that the magnetization directions of the two wires face the contact. In Fig. 2(b), the dark signals in the wider wire appear at the bottom of the edge, while those in the narrower wire concentrate at the nanocontact. On the other hand, in Fig. 2(c), the dark signals in the wider wire concentrate at the nanocontact, while those in the narrower wire gather at the bottom of the edge. The magnetization configurations inferred from the MFM images have been shown by the arrows on the right side of each MFM image. We define the DW of Fig. 2(b) as 90° *A* DW and that of Fig. 2(c) as 90° *B* DW, since the magnetization rotation inside the nanocontact is expected to be nearly 90° as shown in the illustrations of Figs. 2(b) and 2(c). The depinning fields of the DWs were estimated for all the observed samples by repeating a field sweep of $0\rightarrow H\rightarrow0$ *in situ* with increaments of H and the scanning of the MFM image at zero field. The depinning field of the 90° *A* DW and 90° *B* DW were found to be 160 and 110 Oe, respectively. In some of the other samples, we found two other types of DWs [Figs. 2(d) and 2(e)]. The dark signals in the narrower wire in these DWs slightly shift from the center of the nanocontact to the top and no signal appears at the bottom edge. Therefore, the magnetization of the edge of the narrower wire tilts from the wire axis as that of the 90° *B* DW. On the other hand, the signals in the wider wire collect at the top of the edge as shown in Fig. 2(d) and collect at the bottom of the edge as shown in Fig. 2(e). The magnetization configurations inferred from the MFM images in Figs. 2(d) and 2(e) are shown on the right side of the images. We define the DW shown in Fig. 2(d) as 0° DW and that shown in Fig. 2(e) as 180° DW. The depinning fields of these DWs were found to be 110 Oe. This value is the same as that of the 90° *B* DW. The 90° *A* DW also appeared occasionally in the samples where the 0° DW or the 180°

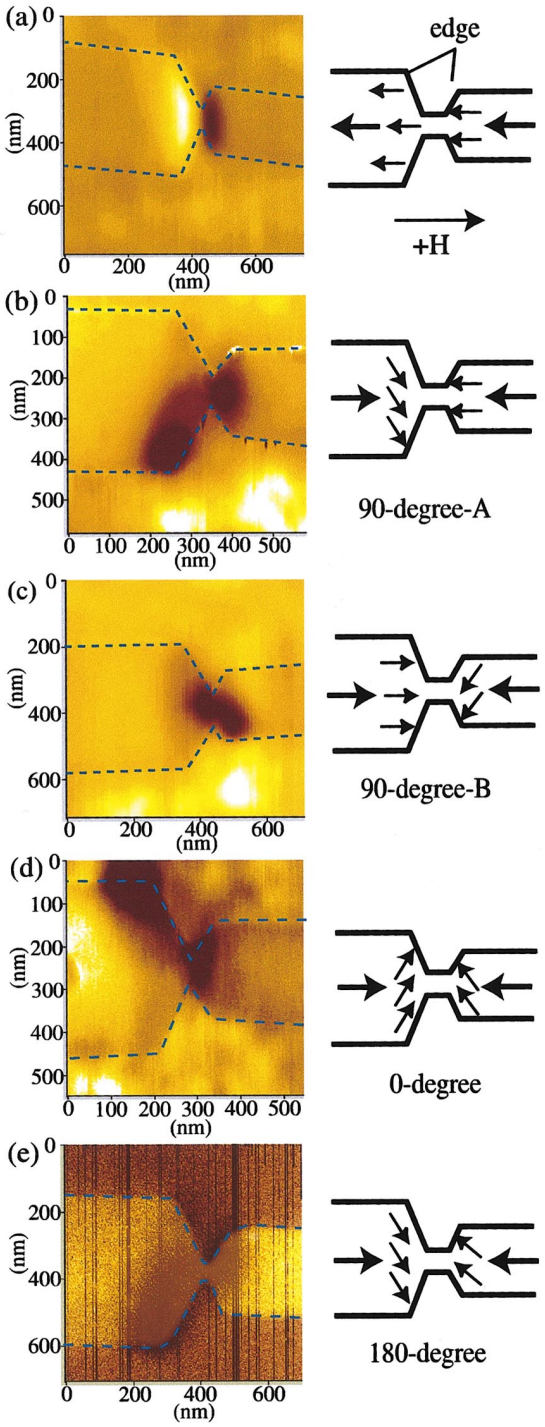

FIG. 2. (Color) MFM images of the area around the nanocontact at remanent magnetization state after fields of (a) −400 Oe→0 Oe and (b) to (e) −400 Oe→+100 Oe were applied. Images (a), (b), and (c) were observed in the same sample. Images (d) and (e) were observed in two other different samples. The magnetizations of the edges rotate from the wire axis or point to the wire axis. The rotation angle of the magnetization in the nanocontact depends on the relative angle of the magnetization of the two edges.

DW was primarily observed. In this manner, the two types of DWs with different depinning fields appeared in the nanocontact in each sample. The combination of the two DWs appearing in repeated measurements was an inherent feature of each sample. The energies of the four DWs are expected to change with the contact size. However, we have not determined the correlation between the contact sizes and the

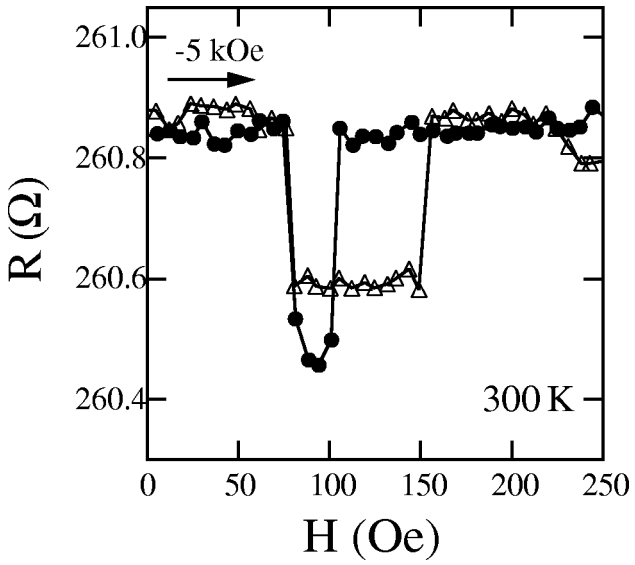

FIG. 3. Two types of MR curves observed at 300 K in the same sample (and with the same saturation field of −5 kOe). The nanocontact size of the sample is 18×38 nm^2.

two appearing DW structures. The appearing DWs are believed to depend on a small difference in the crystalline grain configuration or oxidization in the nanocontact or the edges.

The switching field of the narrower wire for a disconnected sample was also measured using MFM, to be compared with the depinning field of the connected samples. Two types of magnetization configurations of the disconnected edges, which correspond to those in the 0° DW and 180° DW, were found for the same sample at zero field. In both cases, the switching field of the narrower wire was 145 Oe. This value is smaller than 160 Oe and larger than 110 Oe. This implies that the presense of a nanocontact increases the switching field of the narrower wire when the 90° *A* DW is formed, and decreases the switching field when the 90° *B* DW, the 0° DW, or the 180° DW are formed.

B. Magnetoresistance effect

The appearance of two types of DWs was also found in the MR measurement. Prior to the MR measurement, a magnetic field of −5 kOe was applied parallel to the wire axis in order to align the magnetization in one direction and then the field was swept in the counterdirection. We repeatedly measured the MR curves at 300 K. Figure 3 shows the two types of the MR curves between 0 and 250 Oe obtained in the same sample. An abrupt decrease was observed at 80 Oe; the resistance remained almost unchanged until the field reached 110 or 160 Oe, when it abrubtly changed to approximately the same value as that before the decrease at 80 Oe. These fields correspond to the DW injection into the nanocontact and depinning from it, respectively. Since the magnetic fields for the decrease are the same, as shown in Fig. 3, it is concluded that both the types of DWs are nucleated from the pad at the same injection field. The small negative contribution to the resistance by the DW is believed to be due to the anisotropic magnetoresistance (AMR) effect,[10] and the value is consistently explained with the change in resistance of approximately −1% obtained for the field applied perpendicu-

larly to the wire axis. Since the AMR effect depends on the angle between the magnetization and the electric current, it is natural to attribute the difference in values of the resistance change in the two MR curves to the two types of DWs pinned at the nanocontact having different magnetization components to the wire axis. There is also a difference in the depinning field between the two MR curves at 110 and 160 Oe. The values of the resistance change and depinning fields are consistent with the result of MFM observations. Judging from the magnetic structures in Fig. 2, the 90° *A* DW, which has a larger depinning field, is expected to generate a larger resistance value of AMR change than the other three types of DWs, which have a smaller depinning field. It is concluded that the difference between the two MR curves arises from the two DWs pinned at the nanocontact having different magnetic structures and depinning fields. The MR results confirm that the appearance of the two types of DWs in the MFM observations is not an effect of stray fields from the magnetic probe.

C. Micromagnetics simulations

We found two types of DWs with different depinning fields in the same sample. However, some of the related problems have not been solved experimentally. It is not clear why only two DWs out of four appear in each sample. The origin of the different depinning fields for the different DWs is also to be clarified. It is demonstrated in this section that such differences in magnetization processes can be explained by the difference of magnetization configuration inside the nanocontact.

The magnetization configuration inside the nanocontact was not determinable from the MFM observations. The micromagnetics simulation provides information on the stable states of the magnetization configuration of the DW pinned at the nanocontact. Two types of stable states [Figs. 4(a) and 4(b)] were obtained at zero field. These states were given by the calculation starting from different initial magnetization states as schematically illustrated on the right side of Fig. 4. Figure 5 shows the x component and the y component of the magnetization in Fig. 4(a) along the central line of the wire. The z component of all the meshes is nearly zero, which implies that the magnetization rotates in the film plane. In the nanocontact area, the x component is positive and the y component linearly decreases with changing the sign at $x=0$. The profile is similar to a Néel wall with the magnetization rotating from the $+y$ direction to $-y$ direction through the $+x$ direction. The angle of rotation, which is estimated from the magnetization profiles for the y component in Fig. 5(a) around the nanocontact, corresponds to that of a 180° DW of 34 nm thickness. The scale of the magnetization rotation is as small as the size of the nanocontact. In this manner, the magnetic structure inside the nanocontact is characterized by the direction of the rotation of magnetization along the x axis.

In order to easily understand the character of the simulated DW structures, we focus on the magnetization directions of three parts, namely, *W*, *C*, and *N* shown at the top of Fig. 4. The area of *W* is the edge of the wider wire, the area

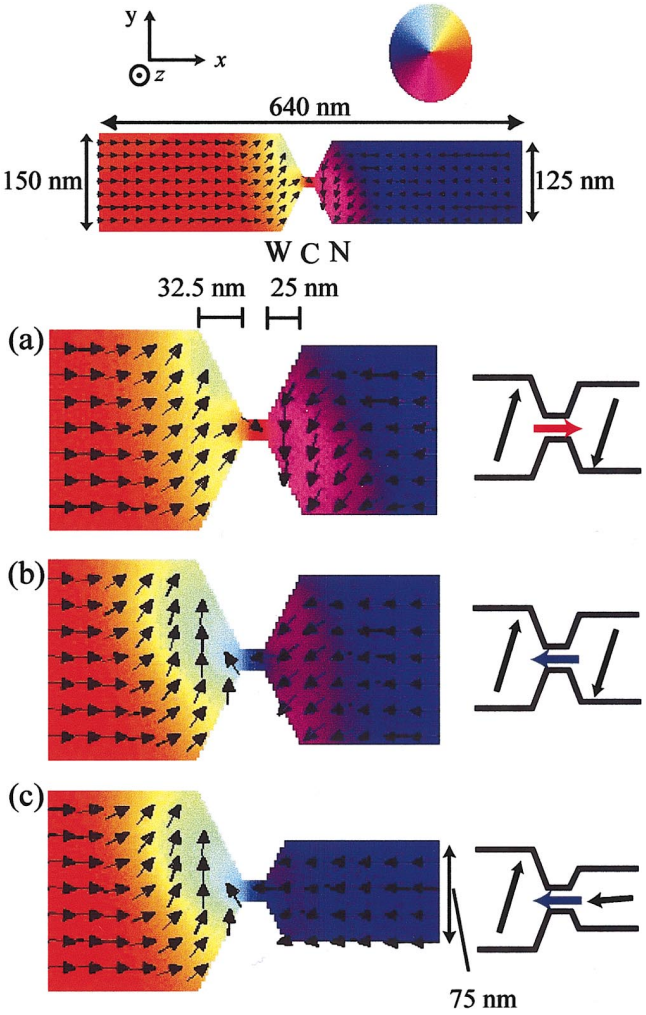

FIG. 4. (Color) The stable states of the DW at zero field on the basis of Landau-Lifshiz-Gilbert (LLG) equations starting from different initial magnetization configurations (shown on the right). Images (a), (b), and (c) are the enlargements around the contact. The wire width of the wire on the right side of the image (c) was narrower (75 nm) than in the images (a) and (b) (125 nm). The arrows and colors represent the direction of the magnetization in the x-y plane. The size of the nanocontact is 20×15 nm^2.

of *C* is the nanocontact, and the area of *N* is the edge of the narrower wire. The magnetizations of *W* and *N* tend to orient perpendicular to the wire axis in order to decrease the demagnetization energy. However, the rotation angles of the magnetization at *W* and *N* differ, depending on the magnetization direction at *C*. If the magnetization at *C* points to the $+x$ direction [Fig. 4(a)], the rotation of the magnetization at *W* perpendicular to the wire axis is suppressed because of the exchange interaction between *W* and *C*. The magnetization rotation of *N* perpendicular to the wire axis is assisted by the exchange interaction between *C* and *N* because the magnetizations at *C* and *N* face with each other. On the other hand, if the magnetization at *C* points to the $-x$ direction [Fig. 4(b)], the magnetization rotation of *W* is assisted and that of *N* is suppressed.

The magnetization rotation of the wire edge next to the nanocontact also depends on the width of the wire. Figure 4(c) shows the magnetization configuration of DW for the sample with a narrower wire, which has a width of 75 nm. The magnetization at *N* does not rotate to the perpendicular

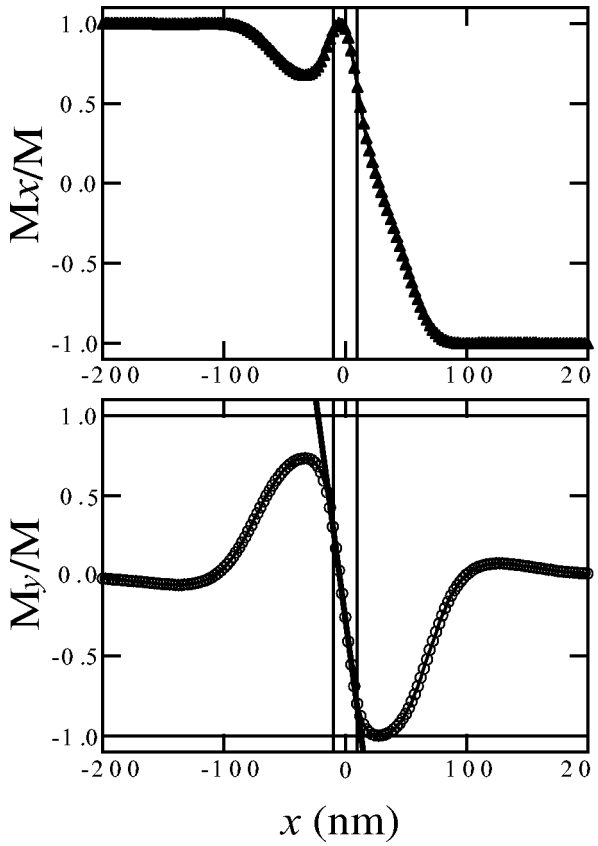

FIG. 5. Magnetization profiles of Fig. 4(a) along the center line of the wire. The DW is confined to the nanocontact. The thin vertical solid lines represent the edges of the nanocontact. The thick solid line represents the linear line fitting for the *y* component of the magnetization from −6.25 to +6.25 nm.

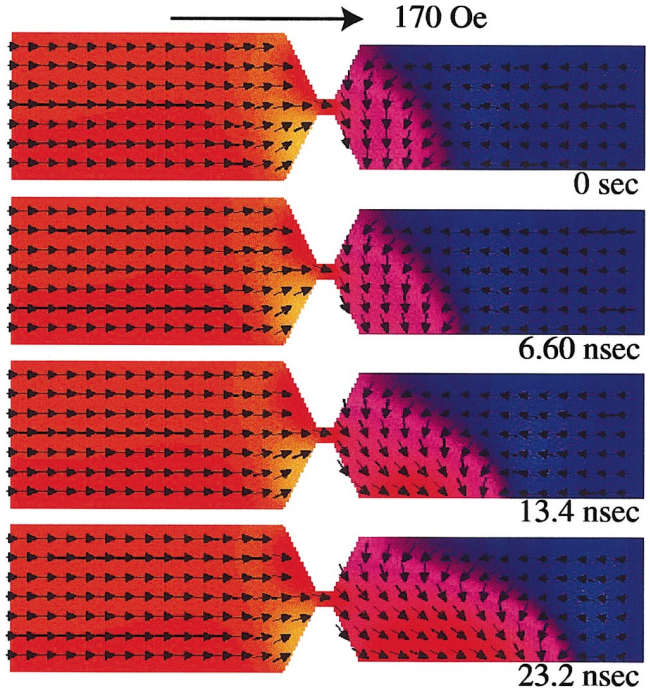

FIG. 6. (Color) Magnetization reversal process of the narrower wire with the DW confined to the nanocontact in Fig. 4(a) at 170 Oe. The perpendicular component of the magnetization to the wire axis at the edge rotates to the wire axis with the application of a field and penetrates into the narrower wire at the depinning field. The penetration process depends on the direction of the magnetization inside the nanocontact. In the case of this figure, the magnetization of the nanocontact assists the magnetization rotation at the edge toward the perpendicular direction to the wire axis since the magnetization of the nanocontact points to the magnetic field.

direction since the shape anisotropy becomes larger with the decrease in wire width. This configuration is considered to correspond to the 90° *A* DW in Fig. 2.

It should be noted that the depinning fields in the simulation of these DWs are considerably different. The depinning fields of the DWs in Figs. 4(a) and 4(b) were calculated to be +170 and +240 Oe, respectively. This difference originates from the *x* component direction of the magnetization in the nanocontact area *C*. Figure 6 shows the depinning process of the DW shown in Fig. 4(a), at 170 Oe. The DW penetrates into the edge of the narrower wire[11] with the magnetization rotating perpendicularly to the wire axis at the edge. The DW is then injected into the narrower wire. When the *x* component of the magnetization in the narrower wire and the nanocontact are antiparallel at the initial stage, the magnetization of the edge is forced to be in a direction perpendicular to the wire axis by the magnetization of the nanocontact. As a result, the depinning field decreases. When the *x* component of magnetization of the narrower wire and the nanocontact are parallel, the magnetization of the nanocontact forces the direction of magnetization of the narrower edge to be toward the wire axis. As a result, the depinning field increases. In other words, the DW confined to the nanocontact biases the switching field of the narrower wire through the exchange interaction. It should be noted that the switching field of the narrower wire for the disconnected sample shows a value between the values of the two depinning fields of the DWs in the connected sample because of the lack of the exchange biasing.

On the basis of these calculations, the two kinds of DWs with different depinning fields in one sample observed by MFM and MR have been considered to be characterized by the difference in the magnetization direction in the nanocontact. The magnetic structures and depinning fields of DWs observed by MFM are explained in the following manner. When the DW propagation from the pad stops before the nanocontact [Fig. 7(a)] with the magnetization at *C* and *N* in the parallel direction, the magnetization at *W* rotates perpendicular to the wire axis and the magnetization *N* remains in the same direction due to the large shape anisotropy of the narrower wire and the exchange interaction between *C* and *N*. As a result, the 90° *A* DW is realized in the remanent magnetization state. When the magnetization of the nanocontact is reversed after the magnetization reversal of the wider wire [Fig. 7(b)], the magnetization at *N* rotates toward the perpendicular direction to the wire axis and the magnetization at *W* rotates to the same direction of *N* (0° DW), rotates to the opposite direction at *N* (180° DW), or retains the direction (90° *B* DW). These differences are expected to arise from a small deviation of the angle of magnetic field or a small difference of the shape anisotropy, which originates from the sample structures. In any case, the depinning field of the DW depends only on the direction of magnetization in the nanocontact.

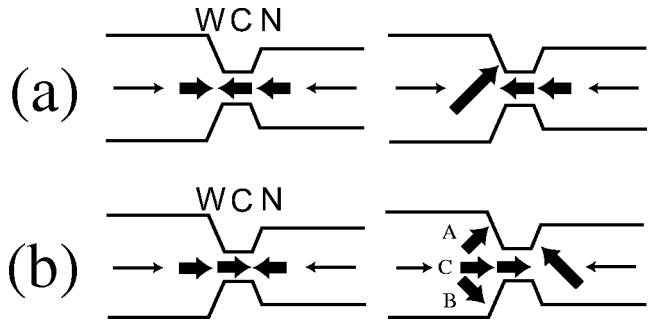

FIG. 7. Schematic illustrations of different magnetization processes occurring around the nanocontact between two wires with different widths. (a) The magnetization reverses to the edge of the wider wire. The magnetization of the edge *W* points a direction perpendicular to the wire axis at a remanent magnetization state. As a result, the magnetization of nanocontact with a $-x$ component is realized. (b) The magnetization reverses until the nanocontact. The magnetization of the edge *N* points to a directionperpendicular to the wire axis and the magnetization of the edge *W* points (A) in the same direction, (B) in the counter direction of *N*, or (C) along the wire axis at a remanent magnetization state. The difference is expected to arise from a small difference of the sample structure and the experimental conditions. As a result, the magnetization of nanocontact with a $+x$ component is realized.

V. SUMMARY

We fabricated nanocontact structures between $Ni_{81}Fe_{19}$ wires using electron-beam lithography and a lift-off process. Two types of DWs pinned at the nanocontact with different magnetic structures and different depinning fields were observed in the same sample in both MFM observations and MR measurements. Micromagnetics simulation showed that a trapped DW at the nanocontact has an internal magnetic structure similar to a Néel wall inside the nanocontact. Two types of DWs with different magnetization directions of the nanocontact are obtained when the injected DW stops before the nanocontact or stops after the nanocontact. The magnetic structures of the DW and the different depinning fields of the DW can be explained by the "exchange biasing" effect between the nanocontact and the narrower wire. In this way, we showed that the magnetization in the nanocontact dominates the magnetization process of connected magnetic elements.

ACKNOWLEDGMENTS

The authors would like to express their gratitude to Dr. Y. Suzuki for valuable discussions. This work was partly supported by Grants-in-Aid for Research for the Future from Japan Society for the Promotion of Science, for Research Assistance from the Asahi Glass Foundation, and for COE Research "Elements Science" from the Ministry of Education, Science, Sports, Culture and Technology of Japan.

[1] P. Bruno, Phys. Rev. Lett. **83**, 2425 (1999).
[2] Y. Labaye, L. Berger, and J. M. D. Coey, J. Appl. Phys. **91**, 5341 (2002).
[3] N. García, M. Muñoz, and Y -W. Zhao, Phys. Rev. Lett. **82**, 2923 (1999).
[4] J. J. Versluijs, M. A. Bari, and J. M. D. Coey, Phys. Rev. Lett. **87**, 026601 (2001).
[5] K. Shigeto, T. Shinjo, and T. Ono, Appl. Phys. Lett. **75**, 2815 (1999).
[6] T. Schrefl, J. Fidler, K. J. Kirk, and J. N. Chapman, J. Magn. Magn. Mater. **175**, 193 (1997).
[7] Y. Yokoyama *et al.*, J. Appl. Phys. **87**, 5618 (2000).
[8] P. P. Freitas and L. Berger, J. Appl. Phys. **57**, 1266 (1985).
[9] A. Yamaguchi, T. Ono, S. Nasu, K. Miyake, K. Mibu, and T. Shinjo, Phys. Rev. Lett. **92**, 077205 (2004).
[10] K. Miyake, K. Shigeto, K. Mibu, T. Shinjo, and T. Ono, J. Appl. Phys. **91**, 3468 (2002).
[11] K. J. Kirk, M. R. Scheinfein, J. N. Chapman, S. McVitie, M. F. Gillies, B. R. Ward, and J. G. Tennan, J. Phys. D **34**, 160 (2001).